

Finite-size scaling for non-linear rheology of fluids confined in a small space

Michio Otsuki*

Department of Pure and Applied Sciences, University of Tokyo, Komaba, Tokyo 153-8902, Japan

(Dated: November 4, 2018)

We perform molecular dynamics simulations in order to examine the rheological transition of fluids confined in a small space. By performing finite-size scaling analysis, we demonstrate that this rheological transition results from the competition between the system size and the length scale of cooperative particle motion.

PACS numbers: 64.70.Pf, 83.10.Rs, 68.15.+e, 47.50.-d

When fluids are confined in a small space, their rheological property changes drastically from that of the fluids in the bulk. A typical example of this rheological transition is observed in a fluid confined between solid walls. When the distance between the walls is so large that the fluid is considered in the bulk, it behaves as a normal Newtonian fluid. On the other hand, when the distance becomes equivalent to that of approximately eight molecular layers, the fluid exhibits an increase in its viscosity, the shear-thinning behavior and the appearance of the yield stress as well as the enhancement of the relaxation time [1]. This rheological transition has been extensively studied by experiments [2, 3] and simulations [4, 5, 6, 7, 8].

Some researchers have conjectured that this rheological transition results from structural transition [5, 6, 7]. However, in some simulations of fluids confined between walls, the rheological transition is observed without any clear structural transition [4]. Hence, we consider that there is another mechanism responsible for this rheological transition.

Let us recall that glassy materials, such as dense colloidal suspensions and super-cooled liquids, also display rheological transition similar to that observed in fluids confined in a small space when the temperature decreases or the density increases [9, 10, 11]. From this fact, we conjecture that fluids confined in a small space and glassy materials have common features [2, 3].

In particular, in glassy materials, it has been observed that the length scale of cooperative particle motion, which is called the dynamical correlation length, becomes comparable with the system size near glass transitions [12, 13]. Therefore, in the case of fluids confined in a small space, the dynamical correlation length might be comparable with the system size when the size is sufficiently small. Our conjecture suggests that the competition between the dynamical correlation length and the system size is an origin of the rheological transition.

In order to test whether the rheological transition is actually caused by the conjectured effect, we investigate a model that does not exhibit any structural transition. By performing numerical simulations with a finite-size scaling analysis [14], we demonstrate that the rheological transition occurs because of the competition between the

system size and the dynamical correlation length.

Model: The system is a 80:20 mixture of Lennard-Jones particles of types A and B in a two-dimensional square box, with an interaction potential

$$V_{\alpha\beta}(\mathbf{r}) = 4\epsilon_{\alpha\beta} \left[\left(\frac{\sigma_{\alpha\beta}}{r} \right)^{12} - \left(\frac{\sigma_{\alpha\beta}}{r} \right)^6 \right], \quad (1)$$

where α and β refer to the two species A and B. In order to restrict crystallization, we investigate the binary mixture. The particles have equal masses, and the interaction parameters are $\epsilon_{AB} = 1.5\epsilon_{AA}$, $\epsilon_{BB} = 0.5\epsilon_{AA}$, $\sigma_{AB} = 0.88\sigma_{AA}$, and $\sigma_{BB} = 0.8\sigma_{AA}$. The length, energy, and time units are expressed in the standard Lennard-Jones units: σ_{AA} (particle diameter), ϵ_{AA} (interaction energy), and $\tau_0 = (m_A \sigma_{AA}^2 / \epsilon_{AA})^{1/2}$, where m_A is the particle mass. The subscript A refers to the major species. We fix the total number density $\rho = N/L^2 = 1.13$, where L is the system size and N is the number of the particles.

The evolution equations of the i -th particle's position $\mathbf{r}_i = (x_i, y_i)$ and velocity $\mathbf{v}_i = (u_i, v_i)$ are numerically integrated by using a leapfrog algorithm with a time step $\delta t = 0.005$. Here, in order to maintain the temperature T , we use the Nose-Hoover algorithm [15]. In order to realize the shear flow $(\gamma y, 0)$ without structural ordering near the boundaries, Lees-Edwards boundary conditions are imposed [15]. Here, γ is the shear rate.

Equilibrium Properties: We first calculate the pair distribution function defined as

$$g(\mathbf{r}) = \frac{L^2}{N^2} \sum_{i \neq j} \langle \delta(\mathbf{r} - \mathbf{r}_i + \mathbf{r}_j) \rangle_{T, \gamma, L}. \quad (2)$$

Here, $\langle \cdot \rangle_{T, \gamma, L}$ represents the ensemble average under the condition that temperature T , the shear rate γ , and the system size L are provided. In Fig. 1, we show the equilibrium pair distribution functions for several values of L when $T = 0.8$ and $\gamma = 0$. It can be seen that the structural transition does not occur when the system size is decreased.

Next, we study the dynamical correlation length $\xi(T)$, following Ref. [12, 13]. For this purpose, we define the local indicator of configuration change as

$$F(\mathbf{r}, t) = \sum_i \delta(\mathbf{r} - \mathbf{r}_i(0)) W(\mathbf{r}_i(t) - \mathbf{r}_i(0)), \quad (3)$$

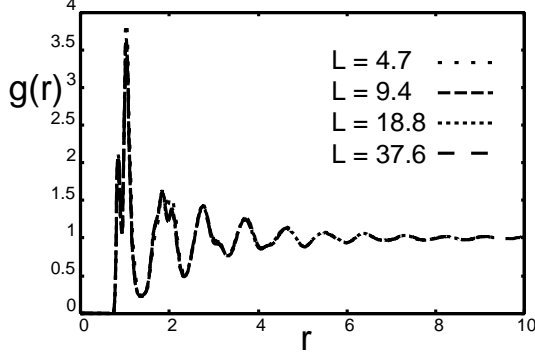


FIG. 1: Pair distribution function $g(\mathbf{r})$ for several values of L when $T = 0.8$ and $\gamma = 0$.

with

$$W(\mathbf{r}) = \begin{cases} 1 & (|\mathbf{r}| < a), \\ 0 & (\text{otherwise}). \end{cases} \quad (4)$$

Here, we choose the value of a as 0.3, which is slightly larger than the square root of the plateau value of the mean square displacement, as discussed in Ref. [12]. Note that $\langle F(\mathbf{r}, t) \rangle$ is akin to the intermediate scattering function when the system is homogeneous. The correlation function $C(\mathbf{r}, t, T)$ of $F(\mathbf{r}, t)$ is defined as

$$C(\mathbf{r}, t, T) = \frac{V^2}{N^2} \langle F(\mathbf{r}, t) F(\mathbf{0}, t) \rangle_{T, \gamma, L} - \frac{V^2}{N^2} \langle F(\mathbf{r}, t) \rangle_{T, \gamma, L}^2. \quad (5)$$

From $C(\mathbf{r}, t, T)$, the amplitude of the correlation is defined as

$$\chi(t, T) = \frac{1}{k_B T} \int d\mathbf{r} C(\mathbf{r}, t, T). \quad (6)$$

In Fig. 2, we show the time dependence of $\chi(t, T)$ for several values of T when $L = 37.6$ and $\gamma = 0$. $\chi(t, T)$ has a maximum value at a time t_{\max} . As the temperature decreases, t_{\max} and the maximum value $\chi(t_{\max}, T)$ increases.

In order to extract $\xi(T)$, we define the Fourier transformation $S(\mathbf{k}, t, T)$ of $C(\mathbf{r}, t, T)$ as

$$S(\mathbf{k}, t, T) = \int d\mathbf{r} C(\mathbf{r}, t, T) \exp(-i\mathbf{k} \cdot \mathbf{r}), \quad (7)$$

where

$$S(0, t, T) = k_B T \chi(t, T). \quad (8)$$

From $S(t, k, T)$, we define $S_{\max}(k, T) = S(k, t_{\max}, T)$. By assuming the functional form of $S_{\max}(k, T)$ as

$$S_{\max}(k, T) = \frac{S_{\max}(0, T)}{1 + (k\xi(T))^2}, \quad (9)$$

we estimate $\xi(T)$ for the case that $\gamma = 0$ and $L = 37.6$. In Fig. 3, $S_{\max}(k, T)/S_{\max}(0, T)$ is displayed as a function of $k\xi(T)$. In Fig. 4, we show $\xi(T)$ as a function of T .

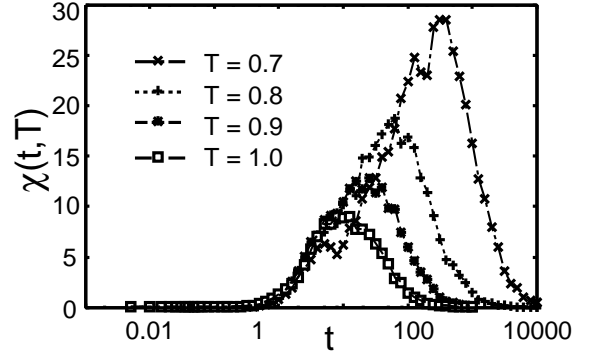


FIG. 2: $\chi(t, T)$ as a function of t for several values of T when $L = 37.6$.

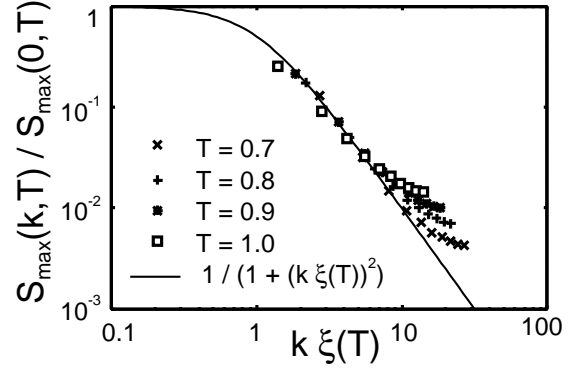


FIG. 3: $S_{\max}(k, T)/S_{\max}(0, T)$ as a function of $k\xi(T)$ for several values of T when $L = 37.6$.

Rheological Properties: As a typical rheological property, we investigate the viscosity. In our system, the shear

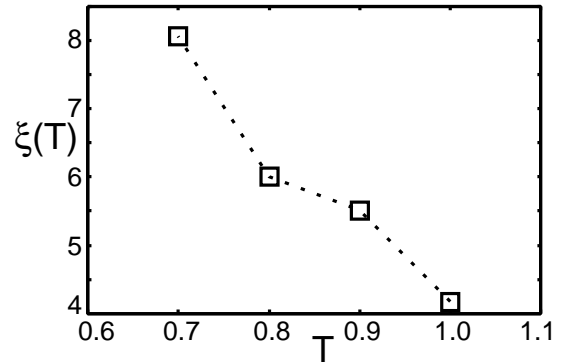


FIG. 4: $\xi(T)$ as a function of T for $L = 37.6$.

stress $\sigma_{xy}(T, \gamma, L)$ is expressed as

$$\sigma_{xy}(T, \gamma, L) = \frac{1}{L^3} \left\langle - \sum_{i=1}^N m_i u_i v_i + \sum_{i \neq j} \frac{x_{ij} y_{ij}}{2r_{ij}} \frac{\partial V(r_{ij})}{\partial r_{ij}} \right\rangle_{T, \gamma, L}, \quad (10)$$

where $x_{ij} = x_i - x_j$, $y_{ij} = y_i - y_j$, and $r_{ij} = |\mathbf{r}_i - \mathbf{r}_j|$ [15]. From $\sigma_{xy}(T, \gamma, L)$ and γ , the viscosity $\eta(T, \gamma, L)$ is defined as

$$\eta(T, \gamma, L) = \frac{\sigma_{xy}(T, \gamma, L)}{\gamma}. \quad (11)$$

In Fig. 5, we show $\eta(T, \gamma, L)$ as a function of γ for several values of T when $L = 37.6$. For $T = 1.0$, the viscosity

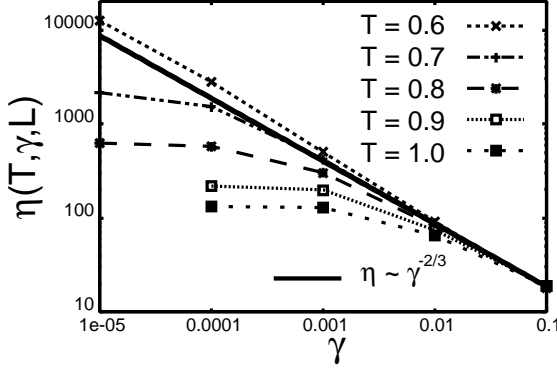


FIG. 5: Relation between η and γ for several values of T when $L = 37.6$.

is independent of the shear rate when $\gamma < 0.001$. This regime is called a Newtonian regime. As the shear rate increases, the viscosity decreases as $\eta \sim \gamma^{-\alpha}$. When the temperature decreases, the Newtonian regime becomes narrower and finally disappears. The exponent $\alpha = 2/3$ is observed in experiments [2] and simulations [4] of thin liquid films. Furthermore, this exponent is observed in simulations of glassy materials [11].

Now, we investigate the system size dependence of the rheological property. As examples, in Fig. 6, we show $\eta(T, \gamma, L)$ as a function of γ for several values of L when $T = 0.6$ and 0.9 . At $T = 0.6$, η changes slightly. On the other hand, when $T = 0.9$, η strongly depends on L in the low shear rate regime as in experiments [2, 3] and simulations [4, 5, 6, 7, 8] of a thin liquid film.

Finite-size scaling: We perform a finite-size scaling analysis in a similar manner to that used for critical phenomena [14]. We first assume the scaling form of the viscosity as

$$\eta(T, \gamma, L) = \eta_0(T, L) G\left(\gamma \cdot \eta_0(T, L)^{\frac{3}{2}}\right), \quad (12)$$

where $\eta_0(T, L)$ is the Newtonian viscosity defined as $\eta_0(T, L) = \lim_{\gamma \rightarrow 0} \eta(T, \gamma, L)$. $G(x)$ is a function having

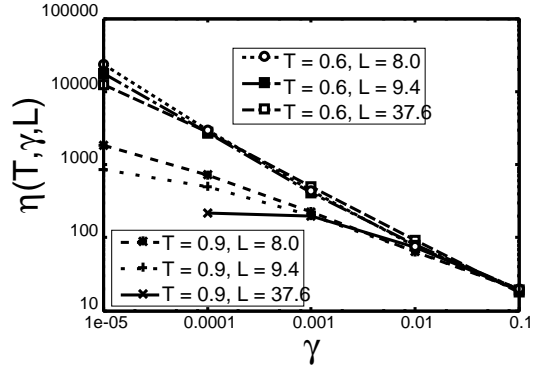


FIG. 6: Relation between the viscosity $\eta(T, \gamma, L)$ and the shear rate γ for several values of L when $T = 0.6$ and 0.9 .

the properties

$$\lim_{x \rightarrow 0} G(x) = 1, \quad (13)$$

$$\lim_{x \rightarrow \infty} G(x) \sim x^{-\frac{2}{3}}. \quad (14)$$

$$(15)$$

It must be noted that this scaling form can be derived from a theory for the rheological property in glassy materials [16]. Here, we only consider the case where $\eta_0(T, L)$ has a finite value. Next, we assume the functional form of $\eta_0(T, L)$ by $\xi(T)$ and L as

$$\eta_0(T, L) = \eta_I(T) H(\xi(T)/L), \quad (16)$$

where $\eta_I(T)$ is the viscosity in the thermodynamical limit $L \rightarrow \infty$ and $H(x)$ is the function having the property

$$\lim_{x \rightarrow 0} H(x) = 1. \quad (17)$$

Then, we test the scaling assumptions described by Eqs. (12) and (16). We show $\eta(T, \gamma, L)/\eta_0(T, L)$ as a function of $\gamma \cdot \eta_0(T, L)^{3/2}$ in Fig. 7. In addition, we show $\eta_0(T, L)/\eta_I(T)$ as a function of $\xi(T)/L$ in Fig. 8. These figures clearly indicate that the scaling assumptions described by Eqs. (12) and (16) are plausible. In addition, the viscosity $\eta_I(T)$ in the thermodynamical limit is shown in the inset of Figs. 8. From these results, we conclude that the size dependence of the rheological property in our system results from the competition between L and $\xi(T)$.

Conclusion and Discussion: We performed the molecular dynamics simulations of the fluid confined in a small space with the Lees-Edwards boundary conditions. In these simulations, we observed the strong size dependence of the rheological property. In addition, we numerically calculated the correlation length $\xi(T)$ of the local configuration change. From the numerical confirmation of the scaling relations given by Eqs. (12) and (16), it has been concluded that the strong size dependence

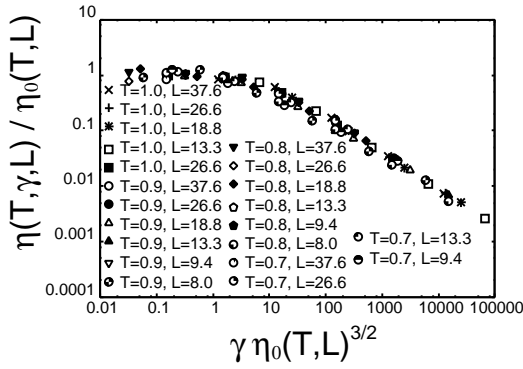


FIG. 7: $\eta(T, \gamma, L) / \eta_0(T, L)$ as a function of $\gamma \cdot \eta_0(T, L)^{3/2}$ for various values of T and system size L .

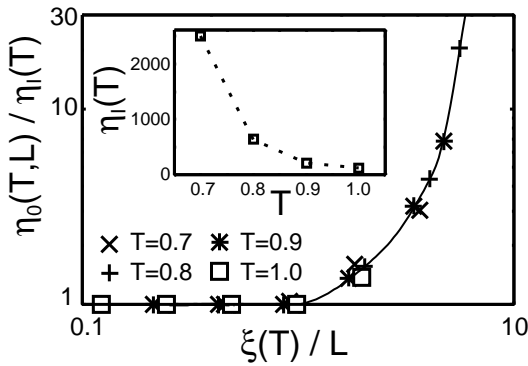


FIG. 8: Main : $\eta_0(T, L) / \eta_I(T)$ as a function of $\xi(T) / L$. Inset : $\eta_I(T)$ as a function of T .

of the rheological property is caused by the competition between the system size and the correlation length.

Although we have shown that the proposed mechanism affects the rheological property in our system without wall boundaries, it is not clear whether it would be really effective in experiments of a thin fluid film with wall boundaries. In such a situation, other effects such as the structural transition might be important for determining the rheological properties.

In Ref. [18], it is shown that the density relaxation time of glassy materials increases when the system size becomes comparable with a dynamical correlation length. With the assumption that the relaxation time is proportional to the viscosity [19], the result in Ref. [18] is similar to the result described by Eq. (16) and Fig. 8. However, we wish to note that in Ref. [18], the rheological property was not studied, and the finite size scaling was not performed.

Finally, let us remind that the correlation length of the

local indicator of the local configuration change, which is the dynamical quantity, is used in our finite-size scaling analysis. This choice is natural because the viscosity is approximately calculated from the time correlation function of the local configuration change [17]. On the other hand, when we recall the fact that the viscosity is calculated from the shear stress, which is the static quantity, it is also expected that the correlation of a static quantity becomes involved in the scaling analysis. However, as far as we have studied, we could not find such a quantity. This problem will be studied in future.

We thank S. Sasa and K. Hukushima for their valuable advice, and H. Tasaki, H. Hayakawa, and T. Hatano for their useful comments.

* Electronic address: otsuki@jiro.c.u-tokyo.ac.jp

- [1] Y.-Z. Hu and S. Granick, *Tribol. Lett.* **5**, 81 (1998).
- [2] H.-W. Hu, G. A. Carson, and S. Granick, *Phys. Rev. Lett.* **66**, 2758 (1991).
- [3] S. Yamada, G. Nakamura, Y. Hanada, and T. Amiya, *Tribol. Lett.* **15**, 83 (2003).
- [4] P. A. Thompson, G. S. Grest, and M. O. Robbins, *Phys. Rev. Lett.* **68**, 3448 (1992).
- [5] A. Jabbarzadeh, P. Harrowell, and R. I. Tanner, *Phys. Rev. Lett.* **96**, 206102 (2006).
- [6] J. Klein and E. Kumacheva, *J. Chem. Phys.* **108**, 6996 (1998).
- [7] S. T. Cui, P. T. Cummings, and H. D. Cochran, *J. Chem. Phys.* **114**, 7189 (2001).
- [8] S. T. Cui, C. McCabe, P. T. Cummings, and H. D. Cochran, *J. Chem. Phys.* **118**, 8941 (2003).
- [9] W. B. Russel, D. A. Saville, and W. R. Schowalter, *Colloidal Dispersions* (Cambridge University Press, New York).
- [10] R. G. Larson, *The Structure and Rheology of Complex Fluids* (Oxford University Press, New York, 1999).
- [11] L. Berthier, and J.-L. Barrat, *J. Chem. Phys.* **116**, 6228 (2002).
- [12] N. Lacevic, F. W. Starr, T. B. Schroder, and S. C. Glotzer, *J. Chem. Phys.* **119**, 7372 (2003).
- [13] L. Berthier, *Phys. Rev. E* **69**, 020201(R) (2004).
- [14] N. Goldenfeld, *Lectures on Phase Transitions and the Renormalization Group* (Addison-Wesley, New York, 1992).
- [15] D. J. Evans and G. Morris, *Statistical Mechanics of Nonequilibrium Liquids*, (Academic, London, 1990).
- [16] M. Otsuki and S. Sasa, *J. Stat. Mech.*, L10004 (2006).
- [17] K. Miyazaki, D. R. Reichman, and R. Yamamoto, *Phys. Rev. E* **70**, 011501 (2004).
- [18] K. Kim, and R. Yamamoto, *Phys. Rev. E* **61**, R41 (2000).
- [19] R. Yamamoto and A. Onuki, *Phys. Rev. E* **58**, 3515 (1998).